Resubmitted to Metallurgical and Materials Transactions A in December 2019

Additive manufacturing of Co-Ni-Ga high-temperature shape memory alloy - Processability and phase transformation behavior

C. Lauhoff[1*], A. Fischer[1], C. Sobrero[2], A. Liehr[1], P. Krooß[1], F. Brenne[1,3], J. Richter[1], M. Kahlert[1], S. Böhm[4], T. Niendorf[1]

[1] *Institute of Materials Engineering, University of Kassel, 34125 Kassel, Germany*
[2] *Institute of Physics Rosario (CONICET), Rosario's National University, 2000 Rosario, Argentina*
[3] *Department of Mechanical Science and Engineering, University of Illinois at Urbana-Champaign Urbana, IL 61801, USA*
[4] *Institute for Production Technologies and Logistics, University of Kassel, 34125 Kassel, Germany*

**corresponding author: lauhoff@uni-kassel.de*

Co-Ni-Ga high-temperature shape memory alloy is additively processed by selective laser melting for the first time. Reversible martensitic transformation of the as-built material is proven by differential scanning calorimetry. Microstructural analysis reveals a columnar-grained microstructure due to epitaxial solidification. Columnar-grained microstructures are characterized by a very low degree of constraints being beneficial for superior functional performance in numerous shape memory alloys. However, process-induced crack formation remains a challenge towards robust realization of adequate mechanical properties.

28 Keywords: High-temperature shape memory alloys, Co-Ni-Ga, Additive manufacturing,
29 Selective laser melting, Columnar grain
30

Binary Ni-Ti is currently the shape memory alloy (SMA) system of choice in many niche applications due to its good biocompatibility, high transformation strains and pronounced cyclic stability. However, Ni-Ti SMAs suffer from limited transformation temperatures (TTs) and high production costs [1–3]. In order to extend the application temperature range, high-temperature (HT-) SMAs featuring increased martensite start temperatures (M_s) have been designed. These alloys enable new applications in the fields of aerospace, automotive, oil and gas as well as other industries [4,5]. Adding a third element to Ni-Ti is a common practice to increase the TTs [4]. Ni-Ti-Hf is currently the most promising HT-SMA being in focus of many studies [6–8]. However, high costs of the alloying elements as well as the highly challenging processing and machining remain major roadblocks towards the widespread use of Ni-Ti-Hf in industrial applications [9,10].

Over the last decades many alternative alloy systems have been introduced as HT-SMA candidates [4,5]. Among the alternative systems, the Heusler-type Co-Ni-Ga alloys have gained considerable attention [11]: Co-Ni-Ga, undergoing a martensitic transformation from cubic B2-ordered austenite to tetragonal $L1_0$ martensite [12], consists of relatively inexpensive alloying elements and features excellent functional properties at elevated temperatures. In single crystalline state, a fully reversible pseudoelastic response up to temperatures of about 500 °C and excellent functional stability at temperatures up to 100 °C have been shown [13–15]. This qualifies Co-Ni-Ga e.g. for high-temperature damping applications. Aging of stress-induced martensite, referred to as *SIM-aging* [16], changes the chemical order and, thus, is suited to directly tailor the TTs. Hence, stable high-temperature actuation can be obtained as well [16,17]. In addition, good formability can be obtained by controlled segregation of the ductile secondary γ-phase (A1) [18–21].

The fundamental properties of this alloy system are well characterized. However, excellent functional properties have been reported mainly for single crystalline material so far. Owing to a pronounced anisotropic transformation behavior and a limited number of martensite variants, deformation constraints at grain boundaries (GB) cannot be sufficiently accommodated in polycrystalline material with random texture. Eventually, premature failure, i.e. intergranular fracture upon thermo-mechanical processing and/or loading is commonly observed [4,19,22]. Even grain boundary engineering via segregation of the highly ductile γ-phase along the GBs is not capable to fully prevent cracking of unfavorable GBs in polycrystalline Co-Ni-Ga structures when martensitic phase transformation occurs [22,23]. Thus, the key towards superior shape memory performance in relatively brittle and anisotropic SMAs is the presence of microstructures, being characterized by a very low degree of grain constraints [24–26]. Triple junctions have been proven to be the most detrimental microstructural feature leading to rapid structural and functional degradation [26]. In line with those findings, a columnar-grained microstructure, featuring a strong ⟨001⟩ texture and geometrically absolutely straight GBs of low-angle character, has been proposed to overcome these issues in case of a Cu-based SMA [27,28]. A different approach aims at realization of oligocrystals, also referred to as bamboo-like structures, in which the GBs exceed the entire cross section of the sample and are mainly oriented perpendicular to the loading axis [24,25]. Despite the obvious differences between both microstructures, i.e. columnar-grained and bamboo-like structures, the low degree of constraints is found to be vital for obtaining superior functional properties in polycrystalline SMAs, being competitive to those of their single crystalline counterparts [19,24,27,29].

Recently, the group of Kainuma introduced a promising cyclic heat treatment in order to control the grain size in SMAs by abnormal grain growth (AGG) [30]. So far, AGG induced by a cyclic

heat treatment has been observed for Cu-Al-Mn [30,31] and Fe-Mn-Al-Ni-X [32,33] SMAs, leading to oligocrystalline grain structures or even single crystals in the range of several centimeters. In a very recent study, a novel thermo-mechanical processing route for obtaining AGG in polycrystalline Co-Ni-Ga HT-SMAs was introduced [20,21]. Hot extrusion followed by a post-processing heat treatment led to the formation of bamboo structures evoking enhanced functional performance. Nonetheless, as processing remains highly challenging, alternative procedures providing for microstructures with minimized grain constraints have to be developed.

In this regard, additive manufacturing (AM) technologies are highly attractive, as these techniques allow for direct microstructure design [34,35]. One of the most common AM techniques for processing of metallic materials is the powder bed based selective laser melting (SLM) method. During SLM, a laser system is used to melt a pre-alloyed powder layer by layer according to data provided by a computer-aided design file. A direct microstructural design is achieved by controlling the thermal gradient and the solidification velocity, which in turn can be adjusted by the processing parameters, such as laser power, scanning velocity, hatch distance and scanning pattern [36]. As has been shown for various materials, strongly textured columnar-grained microstructures can be obtained by SLM processing [36–39]. However, no work has been published on AM of Co-Ni-Ga in literature so far, although direct microstructure design is highly promising for obtaining excellent functional material properties. In order to close this gap, the current study focuses on the SLM processability of a Co-Ni-Ga HT-SMA. Microstructure and martensitic phase transformation behavior of SLM material have been thoroughly investigated. The general feasibility of direct microstructure design, i.e. realization

of a columnar-grained microstructure, is reported. Critical steps towards robust processing of the alloy are highlighted.

In the current study a SLM machine SLM280 ^{HL} employing a 400 W laser was used for fabrication of specimens from a Co-Ni-Ga SMA with a nominal composition of 49Co–21Ni–30Ga (in at.%). This composition is optimized in terms of shape memory properties with a high degree of strain recoverability [15]. The chemical composition of the initial as-cast material was 48.9 Co, 21.0 Ni and 30.1 Ga (in at.%) as determined by X-ray fluorescence analysis (XRF). Co-Ni-Ga SMA powder with a particle size ranging from 20 to 52 µm was obtained by gas atomization of the as-cast material, which was carried out by TLS Technik. Chemical composition of the powder material was determined using energy-dispersive X-ray spectroscopy (EDS). 10×10×15 mm^3 cubes were manufactured with a layer thickness of 50 µm and a hatch distance of 0.12 mm under argon atmosphere at 110°C. The laser operated at a nominal power of 175 W and a scan velocity of 650 mm s^{-1}, resulting in an energy density of 45 J mm^{-3}. A bidirectional scanning strategy with 90° rotation between the successive layers was employed for fabrication of all cubes. In the light of a robust processing as well as the desired microstructure characterized by a low degree of constraints the scanning strategy is suitable to reduce the process-induced residual stresses [40,41] and, concurrently, known to be beneficial for a pronounced texture evolution during processing [36].

The as-built cubes were cut by electrical discharge machining (EDM) along and perpendicular to the building direction (BD). Samples were ground down to 5 µm grit size in order to remove the EDM-affected surface layer. Following grinding, samples were mechanically polished for 1 h using a colloidal SiO_2 suspension with 0.02 µm particle size. For microstructure characterization, optical microscopy (OM) as well as scanning electron microscopy (SEM)

including energy dispersive spectroscopy (EDS) were employed. For OM, samples were etched using a solution of 33 ml ethanol, 8.5 ml H_20, 50 ml HCl and 8.5 g Cu_2S. For phase analysis, synchrotron radiation and a PerkinElmer (XRD1621) area detector were employed at the P02.1 high-resolution powder diffraction beamline (DESY synchrotron facility, Hamburg, Germany). Using synchrotron diffraction sample, volumes of several mm^3 can be probed and a detailed, high-resolution microstructure analysis is enabled. A wavelength of 0.02072926 nm was used. For further details on the synchrotron beamline P02.1 the reader is referred to [42]. Defect analysis in the sample volume was carried out using a Zeiss X-radia 520 Versa micro-computed tomography system (µ-CT) with a sub-micron resolution. For the investigation a sample volume of $2\times2\times4\ mm^3$ was scanned. The µ-CT operated at 80 kV. For analysis a sub-volume of $1750\times1750\times3150\ \mu m^3$ was extracted from the scanned sample volume in order to avoid surface effects. The voxel size was set to 3.9 µm. Differential scanning calorimetry (DSC) was used to investigate the martensitic phase transformation behavior. DSC was conducted using a Mettler-Toledo DSC 1 calorimeter at heating and cooling rates of 10 K min^{-1}.

Figure 1 shows synchrotron diffraction patterns obtained at room temperature from the initial Co-Ni-Ga powder and the SLM as-built condition. The powder particles are fully austenitic with a B2 type ordered bcc lattice, as determined from the peaks at diffraction angles between 4.5° and 13° (Fig.1a). The lattice parameter of the B2 austenite is a = 2.865 Å. The powder particles following gas atomization feature high sphericity and only a small fraction of adhering satellites (inset in Fig.1a). Following AM, the material features a dual-phase microstructure, as can be deduced from the additional peaks in the diffraction pattern (Fig.1b). In addition to the austenitic phase with a = 2.858 Å, tetragonal martensite is present. The crystal structure of the martensitic phase is $L1_0$ with lattice parameters of a = 2.711 Å and c = 3.170 Å. All lattice

parameters are in accordance to literature [12,43]. The slight deviation between the austenitic lattice parameters can be attributed to process-induced residual stresses and minor changes in chemical composition, as will be detailed hereafter. The dual-phase microstructure appears as a lath like austenite-martensite relief in the individual grains similar to that of as-cast Co-Ni-Ga alloys in [44,45] (s. inset in Fig.1b).

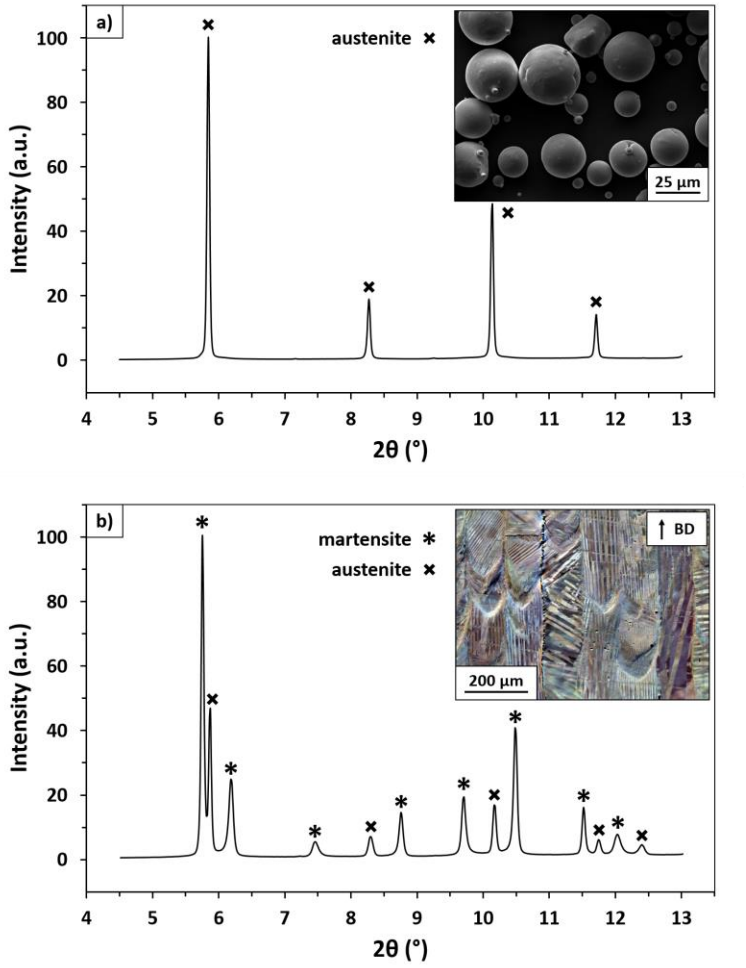

Figure 1: Synchrotron diffraction patterns of (a) Co-Ni-Ga powder and (b) the SLM processed material in the as-built condition. The SEM and Argus image in the insets show the powder particles (a) and the as-built microstructure (b), respectively.

The optical micrographs in Figure 2a and b depict the microstructure of the as-built material parallel and perpendicular to BD, respectively. Columnar grains with long axes in the millimeter range grow parallel to BD (Fig.2a). Owing to the partial re-melting of the underlying solid material, epitaxial solidification occurs during the SLM process [36,38] so that the resulting grain long axes are clearly larger than the initial layer thickness. Although epitaxial grain growth across individual layers was reported for various SLM fabricated materials [36–39,46,47], the strong columnarity of the as-built Co-Ni-Ga is remarkable. This is further highlighted by the grain structure resolved perpendicular to BD (Fig.2b). Due to the bidirectional scanning strategy in combination with the 90° rotation applied, a clear checkerboard like grain arrangement is formed, as also observed in e.g. [38,47] for Ta and Ni-Ti, respectively. Liu et al. [27,28] found an almost perfect pseudoelastic behavior in columnar-grained microstructures with strong crystallographic texture and absolutely straight low-energy GBs in Cu-based SMAs. In addition, even if no strong texture is present, enhanced functional properties and excellent resistance against GB cracking were shown by the current authors in a very recent study for both bamboo-like and columnar-grained Co-Ni-Ga bi-crystals [22]. Consequently, additive manufacturing via SLM is thought to be highly promising to obtain Co-Ni-Ga HT-SMAs with appropriate microstructures featuring excellent resistivity to functional and structural degradation.

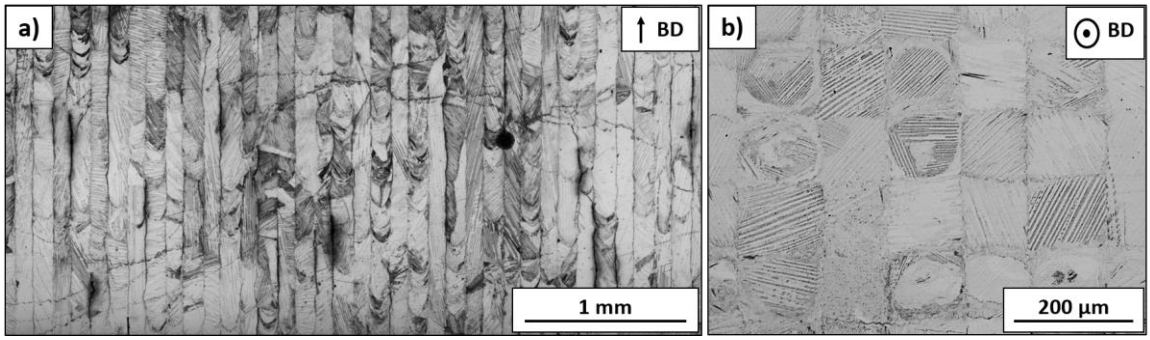

Figure 2: *Optical micrographs revealing the microstructure of Co-Ni-Ga processed by SLM in the as-built condition. The images represent the side view (a) and the top view (b) of the manufactured cubes, as indicated by the arrows labelled* BD.

Results from µ-CT shown in Figure 3 reveal substantial crack formation in the columnar-grained SLM Co-Ni-Ga. A relative density of 85.6% has been determined from these results. It has to be noted that in a preceding laser parameter study material of significantly higher density, i.e. free of cracks, was obtained. However, those conditions were characterized by an unfavorable globular and fine-grained microstructure (not shown). For the sake of brevity, only the set of processing parameters leading to favorable microstructural features is presented in this paper. The cracks depicted in Figure 3 are mainly oriented parallel to the laser scanning vectors during processing. The reason for this phenomenon is seen to be rooted in residual stresses, which typically are formed due to repeated heating, solidification and cooling during layer-wise processing [48], leading to phenomena such as hot and cold cracking. In addition, owing to the high cooling rates within the process, precipitation of the ductile secondary γ-phase along the GBs is not observed, as can be deduced from the synchrotron analysis (Fig.1b) and the optical micrographs (Fig.2). This phase has been proven to be of highest importance to hinder intergranular crack nucleation and propagation [22,23]. The unfavorable combination of the thermally induced stresses and the high brittleness of the as-built material probably leads to cracking alongside the GBs during the SLM process. A parameter optimization including base plate heating up to 600°C is currently considered in order to obtain crack free material which simultaneously shows the desired microstructural features. Increasing the base plate temperature is seen to be very promising to reduce the process induced residual stresses in hard

196 to process alloys, e.g. tool steels [50]. Furthermore and in light of the cost efficiency of the AM
197 process, the adjustment of the process related parameters in order to avoid process induced
198 defects should be in focus of future work instead of using well-established post process
199 treatment procedures, such as hot isostatic pressing (HIP). However, further process parameter
200 optimization is clearly beyond the scope of present work.
201

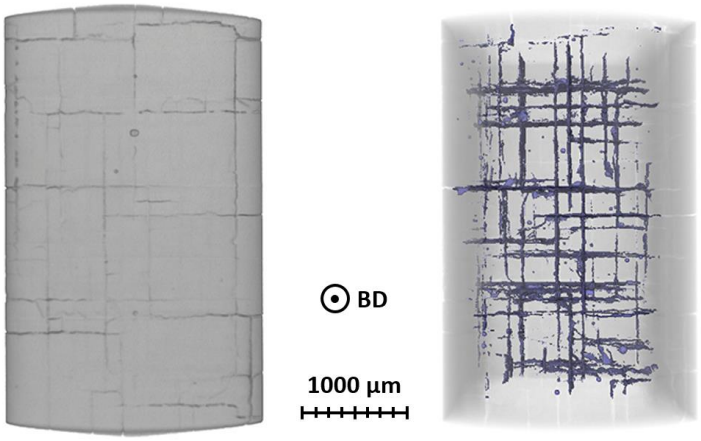

202
203 *Figure 3: Computed tomography analysis of as-built Co-Ni-Ga showing substantial crack*
204 *formation after SLM fabrication: 2D image of a single plane (left), 3D visualization (right).*
205
206 The thermal phase transformation characteristics of as processed Co-Ni-Ga, revealed by DSC
207 analysis, are shown in Figure 4. The endothermic and exothermic reactions associated with the
208 forward and reverse martensitic transformation can be clearly identified in the DSC curve upon
209 heating and cooling, respectively. The TTs of the as-built condition, determined using the
210 tangent method, were found to be M_s=77°C, M_f=34°C, A_s=50°C and A_f=95°C. It is important to
211 note that the synchrotron phase analysis (Fig.1b) and the optical micrographs (Fig.2) of the as-
212 built material revealed an austenitic-martensitic dual-phase microstructure at room temperature,
213 i.e. M_f below RT. The slight difference in TTs to the DSC results (M_f=34°C) could be due to

minor inhomogeneity in the microstructure, slight differences in local chemical composition and/or internal stress state [49]. At this point it has to be emphasized that the material utilized in this study was not homogenized after SLM processing. In addition, specimens for DSC had to be cut and polished, at least leading to change of residual stress state. Quantitative evaluation of the impact of each single parameter, however, is clearly beyond the scope of the present study and, thus, has to be subject of future work.

Still, the DSC results indicate that the absolute TTs as well as the temperature ranges for forward and reverse transformation, i.e. $\Delta_1=A_f - A_s$ and $\Delta_2=M_s - M_f$, are increased compared to single crystalline $Co_{49}Ni_{21}Ga_{30}$ [49]. The increase of Δ_1 and Δ_2 is mainly attributed to the polycrystalline state and grain constraints, respectively. The increase in TTs is thought to be rooted in a general change in chemical composition. Increased Ni and decreased Ga contents have been reported to lead to higher M_s in the Co-Ni-Ga system [44,51]. In the present study the Ga content in the as-built material was found to be about 1.0 at. % below that of both the initial as-cast as well as the powder material (as determined by EDS). Thus, the increase in TTs is mostly attributed to the evaporation of the volatile element Ga during SLM processing. As shown by Elahinia et al. [8] for a Ni-Ti-Hf HT-SMA, evaporation of nickel and oxygen pick are very influential to the transformation behavior. Further factors contributing the shift of TTs and the increase of the transformation temperature ranges Δ_1 and Δ_2 (as compared to the single crystalline material) might be process-induced defects, such as inclusions and cracks shown for Ni-Ti [52], the latter ones being very prominent in the microstructure under investigation. In contrast to the Ni-Ti-based alloys being very sensitive to the alloy composition in terms of the TTs, however, adequate post heat treatments seem to offer more efficient pathways for property optimization in Co-Ni-Ga [16,17,44].

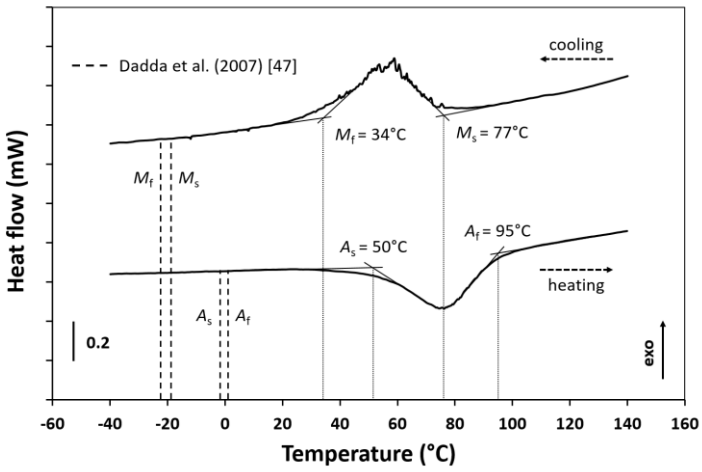

Figure 4: DSC curve for SLM Co-Ni-Ga in the as-built condition. The characteristic transformation temperatures upon heating (A_s and A_f) and cooling (M_s and M_f) are marked. In addition, transformation temperatures of single crystalline $Co_{49}Ni_{21}Ga_{30}$ recompiled from Ref. [49] are highlighted by dashed lines.

In conclusion, the current study demonstrates for the first the time the processability of Co-Ni-Ga HT-SMAs via SLM. Reversibility of the martensitic transformation and characteristic TTs have been shown by DSC. By choosing a suitable set of processing parameters a favorable microstructure is obtained directly after processing. Epitaxial growth leads to an anisotropic, columnar microstructure being very attractive for enhanced functional properties in polycrystalline SMA systems. Thus, it is expected that additive manufacturing of hard to form Co-Ni-Ga will open up new possibilities to overcome major roadblocks toward application. Avoidance of severe processing induced defects needs to be addressed in future studies in order to evaluate the thermo-mechanical functional properties in more detail.

Financial support by Deutsche Forschungsgemeinschaft (Project No. 250216343; NI1327/7-3) within the Emmy Noether-Program is gratefully acknowledged. DESY (Hamburg, Germany), a member of the Helmholtz Association HGF, is thanked for the provision of experimental facilities at the photon beamline P02.1 and the support laboratory. The authors gratefully acknowledge the assistance of Christian Staab with the DSC experiments.

References

[1] K. Otsuka, C.M. Wayman: Shape memory materials, Cambridge University Press, Cambridge, 1999.
[2] K. Otsuka, X. Ren: Prog. Mater Sci., 2005, vol. 50, pp. 511–678.
[3] D.C. Lagoudas: Shape memory alloys, Springer, Boston, MA, 2008.
[4] J. Ma, I. Karaman, R.D. Noebe: Int. Mater. Rev., 2013, vol. 55, pp. 257–315.
[5] G.S. Firstov, J. van Humbeeck, Y.N. Koval: Mater. Sci. Eng., A, 2004, vol. 378, pp. 2–10.
[6] H. Sehitoglu, L. Patriarca, Y. Wu: Curr. Opin. Solid State Mater. Sci., 2017, vol. 21, pp. 113–20.
[7] H. Sehitoglu, Y. Wu, L. Patriarca: Scr. Mater., 2017, vol. 129, pp. 11–15.
[8] M. Elahinia, N. Shayesteh Moghaddam, A. Amerinatanzi, S. Saedi, G.P. Toker, H. Karaca, G.S. Bigelow, O. Benafan: Scr. Mater., 2018, vol. 145, pp. 90–94.
[9] D. Biermann, F. Kahleyss, E. Krebs, T. Upmeier: J. of Materi Eng and Perform, 2011, vol. 20, pp. 745–51.
[10] M.H. Wu: Mater. Sci. Forum, 2002, vol. 394-395, pp. 285–92.
[11] K. Oikawa, T. Ota, F. Gejima, T. Ohmori, R. Kainuma, K. Ishida: Mater. Trans., 2001, vol. 42, pp. 2472–75.
[12] A. Reul, C. Lauhoff, P. Krooß, M.J. Gutmann, P.M. Kadletz, Y.I. Chumlyakov, T. Niendorf, W.W. Schmahl: Shap. Mem. Superelasticity, 2018, vol. 4, pp. 61–69.
[13] P. Krooß, T. Niendorf, P.M. Kadletz, C. Somsen, M.J. Gutmann, Y.I. Chumlyakov, W.W. Schmahl, G. Eggeler, H.J. Maier: Shap. Mem. Superelasticity, 2015, vol. 1, pp. 6–17.
[14] J.A. Monroe, I. Karaman, H.E. Karaca, Y.I. Chumlyakov, H.J. Maier: Scr. Mater., 2010, vol. 62, pp. 368–71.
[15] J. Dadda, H.J. Maier, I. Karaman, H.E. Karaca, Y.I. Chumlyakov: Scr. Mater., 2006, vol. 55, pp. 663–66.
[16] T. Niendorf, P. Krooß, C. Somsen, G. Eggeler, Y.I. Chumlyakov, H.J. Maier: Acta Mater., 2015, vol. 89, pp. 298–304.
[17] C. Lauhoff, P. Krooß, D. Langenkämper, C. Somsen, G. Eggeler, I. Kireeva, Y.I. Chumlyakov, T. Niendorf: Funct. Mater. Lett., 2018, vol. 11, pp. 1850024.
[18] E. Dogan, I. Karaman, Y.I. Chumlyakov, Z.P. Luo: Acta Mater., 2011, vol. 59, pp. 1168–83.

[19] M. Vollmer, P. Krooß, C. Segel, A. Weidner, A. Paulsen, J. Frenzel, M. Schaper, G. Eggeler, H.J. Maier, T. Niendorf: J. Alloys Compd., 2015, vol. 633, pp. 288–95.
[20] E. Karsten, G. Gerstein, O. Golovko, A. Dalinger, C. Lauhoff, P. Krooss, T. Niendorf, A. Samsonenko, H.J. Maier: Shap. Mem. Superelasticity, 2019, vol. 5, pp. 84–94.
[21] T. Niendorf, C. Lauhoff, E. Karsten, G. Gerstein, A. Liehr, P. Krooß, H.J. Maier: Scr. Mater., 2019, vol. 162, pp. 127–31.
[22] C. Lauhoff, M. Vollmer, P. Krooß, I. Kireeva, Y.I. Chumlyakov, T. Niendorf: Shap. Mem. Superelasticity, 2019, vol. 5, pp. 73–83.
[23] R.D. Dar, H. Yan, Y. Chen: Scr. Mater., 2016, vol. 115, pp. 113–17.
[24] Y. Sutou, T. Omori, R. Kainuma, K. Ishida: Acta Mater., 2013, vol. 61, pp. 3842–50.
[25] S.M. Ueland, Y. Chen, C.A. Schuh: Adv. Funct. Mater., 2012, vol. 22, pp. 2094–99.
[26] S.M. Ueland, C.A. Schuh: J. Appl. Phys., 2013, vol. 114, pp. 53503.
[27] J.-L. Liu, H.-Y. Huang, J.-X. Xie: Mater. Des, 2014, vol. 64, pp. 427–33.
[28] J.-L. Liu, H.-Y. Huang, J.-X. Xie, S. Xu, F. Li: Scr. Mater., 2017, vol. 136, pp. 106–10.
[29] T. Omori, M. Okano, R. Kainuma: APL Mater., 2013, vol. 1, pp. 32103.
[30] T. Omori, T. Kusama, S. Kawata, I. Ohnuma, Y. Sutou, Y. Araki, K. Ishida, R. Kainuma: Science, 2013, vol. 341, pp. 1500–02.
[31] T. Kusama, T. Omori, T. Saito, S. Kise, T. Tanaka, Y. Araki, R. Kainuma: Nat. Commun., 2017, vol. 8, pp. 354.
[32] T. Omori, H. Iwaizako, R. Kainuma: Mater. Des, 2016, vol. 101, pp. 263–69.
[33] M. Vollmer, T. Arold, M.J. Kriegel, V. Klemm, S. Degener, J. Freudenberger, T. Niendorf: Nat. Commun., 2019, vol. 10, pp. 2337.
[34] T. Niendorf, F. Brenne, M. Schaper, A. Riemer, S. Leuders, W. Reimche, D. Schwarze, H.J. Maier: Rapid Prototyp. J., 2016, vol. 22, pp. 630–35.
[35] T. Niendorf, S. Leuders, A. Riemer, F. Brenne, T. Tröster, H.A. Richard, D. Schwarze: Adv. Eng. Mater., 2014, vol. 16, pp. 857–61.
[36] L. Thijs, K. Kempen, J.-P. Kruth, J. van Humbeeck: Acta Mater., 2013, vol. 61, pp. 1809–19.
[37] T. Niendorf, S. Leuders, A. Riemer, H.A. Richard, T. Tröster, D. Schwarze: Metall and Materi Trans B, 2013, vol. 44, pp. 794–96.
[38] L. Thijs, M.L. Montero Sistiaga, R. Wauthle, Q. Xie, J.-P. Kruth, J. van Humbeeck: Acta Mater., 2013, vol. 61, pp. 4657–68.
[39] F. Brenne, A. Taube, M. Pröbstle, S. Neumeier, D. Schwarze, M. Schaper, T. Niendorf: Prog. Addit. Manuf., 2016, vol. 1, pp. 141–51.
[40] T. Simson, A. Emmel, A. Dwars, J. Böhm: Addit. Manuf., 2017, vol. 17, pp. 183–89.
[41] M.F. Zaeh, G. Branner: Prod. Eng. Res. Devel., 2010, vol. 4, pp. 35–45.
[42] A.-C. Dippel, H.-P. Liermann, J.T. Delitz, P. Walter, H. Schulte-Schrepping, O.H. Seeck, H. Franz: J. Synchrotron Radiat., 2015, vol. 22, pp. 675–87.
[43] P.M. Kadletz, P. Krooß, Y.I. Chumlyakov, M.J. Gutmann, W.W. Schmahl, H.J. Maier, T. Niendorf: Mater. Lett., 2015, vol. 159, pp. 16–19.
[44] J. Liu, M. Xia, Y. Huang, H. Zheng, J. Li: J. Alloys Compd., 2006, vol. 417, pp. 96–99.
[45] M. Wuttig, J. Li, C. Craciunescu: Scr. Mater., 2001, vol. 44, pp. 2393–97.

[46] L. Thijs, F. Verhaeghe, T. Craeghs, J. van Humbeeck, J.-P. Kruth: Acta Mater., 2010, vol. 58, pp. 3303–12.
[47] T. Bormann, B. Müller, M. Schinhammer, A. Kessler, P. Thalmann, M. de Wild: Mater. Charact., 2014, vol. 94, pp. 189–202.
[48] P. Mercelis, J.-P. Kruth: Rapid Prototyp. J., 2006, vol. 12, pp. 254–65.
[49] J. Dadda, D. Canadinc, H.J. Maier, I. Karaman, H.E. Karaca, Y.I. Chumlyakov: Philos. Mag., 2007, vol. 87, pp. 2313–22.
[50] B. Breidenstein, F. Brenne, L. Wu, T. Niendorf, B. Denkena: HTM J. Heat Treatm. Mat., 2018, vol. 73, pp. 173–86.
[51] K. Oikawa, T. Ota, Y. Imano, T. Omori, R. Kainuma, K. Ishida: JPED, 2006, vol. 27, pp. 75–82.
[52] M. Speirs, B. van Hooreweder, J. van Humbeeck, J.-P. Kruth: J. Mech. Behav. Biomed. Mater., 2017, vol. 70, pp. 53–59.

Autorenversion von: Lauhoff, C., Fischer, A., Sobrero, C. et al. Additive Manufacturing of Co-Ni-Ga High-Temperature Shape Memory Alloy: Processability and Phase Transformation Behavior. Metall Mater Trans A 51, 1056–1061 (2020). https://doi.org/10.1007/s11661-019-05608-z